Orientation-dependent retarding force of a three-dimensional degenerate electron gas for slow homonuclear trimers

Orkhan Osmani[1] and István Nagy[1,2]

[1]*Donostia International Physics Center DIPC, P. Manuel de Lardizabal 4, E-20018 San Sebastián, Spain*

[2]*Department of Theoretical Physics, Institute of Physics, Technical University of Budapest, H-1521 Budapest, Hungary*

(Received 19 June 2012; published 4 October 2012)

A theoretical study is presented on the orientation-dependent retarding force experienced by a slow homonuclear linear trimer moving at arbitrary alignment with the direction of its flight in a three-dimensional degenerate electron gas of metallic densities. We apply a standard multiple-scattering method for elastic scattering of independent electrons off a three-center system in a screening environment. These centers are modeled by short-range auxiliary potentials and thus they are characterized by an effective s-type phase shift η. Within this framework for the orientation-dependent retarding force, the interplay of wave interference and multiple scattering is analyzed in a comparative manner for a realistic set of the input parameters. By allowing a restricted variation in the polar angle between the linear multicenter orientation and its velocity direction, a reasonable agreement with data obtained by a slow carbon trimer is established.

DOI: 10.1103/PhysRevA.86.042901 PACS number(s): 34.50.Bw

I. INTRODUCTION AND MOTIVATION

A recent experimental study [1] on stopping power, conducted with slow C_2^+ and C_3^+ ions traversing self-supporting carbon-foil targets without fragmentation, shows notable negative proximity effects. This effect, characterizing deviations from stopping additivity, is the conventional stopping-power (S) ratio R_N, reading

$$R_N = \frac{1}{N}\frac{S_N}{S_1} \tag{1}$$

for an N-atomic homonuclear intruder moving at a given velocity. The data [1] result in values of about $R_2 = (1/2)$ and $R_3 = (2/3)$. These numbers provide a further definite measure for the so-called efficiency ratio via

$$\mathcal{R}_{N,M} \equiv \frac{S_N}{S_M}, \tag{2}$$

of separate trimer ($N = 3$) and dimer ($M = 2$) stopping powers. One gets $\mathcal{R}_{3,2} = 2$ using data. Thus, an independent-atom model for slow composite intruders is far from reality, since it would give values of $R_2 = R_3 = 1$ and $\mathcal{R}_{3,2} = (3/2)$. The applicability of an united-atom model, where $S_N \propto N^2$, is also questionable in our case, since it would result in $R_2 = 2$ and $R_3 = 3$, and thus in $\mathcal{R}_{3,2} = (3/2)^2 > 2$. Clearly, one should go beyond *these* models that are, according to Sigmund, mostly qualitative and based on intuitive arguments [2].

However, already with a monatomic trimer one has to select possible molecular geometries for the penetrating objects which are reasonable [3–5] not only from the energetic but, equally importantly, from the allowed-space point of view as well. The aim of this theoretical study is to investigate the capability of a treatment for linear trimers, by extending a nonperturbative method applied [6] to interpret the data [1,7–9] for C_2^+ and $H_2{}^+$. That theory gave remarkable agreement with independent experimental findings with these intruders.

Thus, in this work, we consider a linear intact trimer which moves with a given low speed in the direction of its velocity vector through carbon foils. The target is modeled [10] as a degenerate electron gas of fixed density n_0. This *a priori* presumed linearity of a traversing trimer would correspond to a complete-alignment situation. As was pointed out by Arista [10], a well-aligned case at low velocities could be due to coherent multiple scattering of intruder constituents with target atoms. This orienting mechanism in penetration seems to be a reasonable one in those cases where the composite intruder (with strong interatomic binding) and the target consist of the same type of atoms, as in the case with carbon.

Before presenting the details of our approximation in Sec. II, we are tempted to interpret the experimental [1] findings based on the theoretical results obtained [6] for carbon dimers. Since the aligned-dimer stopping power was almost perfectly equal to the stopping power of a single carbon atom, in nice harmony with the experiment, we may image a perfect shadow for the second atom behind the leading one. But a simple extension of this classical shadow picture to the third constituent (see the solid curve in Fig. 2 of Sec. II B) of a linear trimer would give an $R_3 = 1/3$ estimation, with $\mathcal{R}_{3,2} = 1$. On the other hand, by treating the trimer stopping as a formal *sum* of two independent dimer stoppings, we would get $R_3 = (2/3)$ and $\mathcal{R}_{3,2} = 2$ ratios. To understand, at least partially, the physics behind this perfect estimation we extend our method [6] to the case of linear-trimer intruders.

The rest of the paper is organized as follows. Section II is devoted to the theoretical details and the obtained results. These results are discussed in a comparative manner, by exhibiting them in illustrative figures as well. Finally, Sec. III contains our summary and an outlook. Hartree atomic units, $\hbar = m_e = e^2 = 1$, are used throughout.

II. THEORY AND RESULTS

As in the previous work [6] for carbon dimers, we use a well-known [11,12] theoretical framework in order to get the complex scattering amplitude $F_{\mathbf{k},\mathbf{k}'}$ for elastic ($|\mathbf{k}| = |\mathbf{k}'| = k_F$) electron scattering off the field of a slow linear homonuclear trimer. Considering the outgoing part of the scattered-electron wave function, we can write

$$\frac{1}{f} F_{\mathbf{k},\mathbf{k}'} = \Phi_1 e^{i\mathbf{k}'\cdot\mathbf{d}} + \Phi_2 + \Phi_3 e^{-i\mathbf{k}'\cdot\mathbf{d}}, \tag{3}$$

in terms of the complex single-center scattering amplitude $(1/f) \equiv ik(1 + i\cot\eta)$. The positions $(\mathbf{r}_l)$ of trimer constituents $(l = 1,2,3)$ are measured, conveniently [13], from the middle-atom position $\mathbf{r}_2 = 0$, as $(\mathbf{r}_2 - \mathbf{r}_1) = \mathbf{d}$ and $(\mathbf{r}_2 - \mathbf{r}_3) = -\mathbf{d}$. The effective phase shift $\eta(k_F)$ will be fixed below. The complex Φ_l functions encode the important modulating effects of multiple scattering. They are the solutions [6,12] of coupled algebraic equations

$$\Phi_l = e^{i\mathbf{k}\cdot\mathbf{r}_l} + f\sum_j \Phi_j \frac{e^{ik|\mathbf{r}_l-\mathbf{r}_j|}}{|\mathbf{r}_j - \mathbf{r}_l|}, \tag{4}$$

with the obvious constraints of $j \neq l$ and $1 \leqslant l \leqslant 3$ in our case, where $\mathbf{r}_2 = 0$. In the simple impulse approximation, in which positions of $\mathbf{r}_1 = -\mathbf{d}$ and $\mathbf{r}_3 = \mathbf{d}$ are considered in Eq. (4) only at $d \to \infty$, the solutions for Φ_l are plane waves, i.e., they are given by the first terms of the above equation. In such a case, the resulting (approximate) amplitude in Eq. (3) is a simple superposition of plane waves. This decoupling at $d \to \infty$ allows an analytical evaluation of the corresponding perturbative stopping, as we will show below in Eqs. (8) and (9). Beyond this approximation, the $a_{1,2} = a_{2,3} \equiv e^{ikd}/d$ and $a_{1,3} \equiv e^{i2kd}/(2d)$ complex quantities encode the important effect of multiple scattering at realistic values of d.

The orientation-dependent stopping power of an electron gas, i.e., the retarding force in the velocity direction of slow $(v < v_F)$ linear trimers is determined [14,15] from

$$S(\alpha) = n_0\, k_F\, v\,[\cos^2(\alpha)\,\sigma_{\rm tr}^{\parallel}(k_F) + \sin^2(\alpha)\,\sigma_{\rm tr}^{\perp}(k_F)], \tag{5}$$

in terms of the parallel $(\parallel)$ and perpendicular $(\perp)$ transport cross sections. The density of the degenerate electron gas is $n_0 = k_F^3/(3\pi^2)$, and α is the polar angle between the linear-trimer orientation and its velocity direction. The perpendicular force component which may lead to trajectory deflection [14] is proportional to $[\sigma_{\rm tr}^{\parallel}(k_F) - \sigma_{\rm tr}^{\perp}(k_F)]\sin\alpha\cos\alpha$. This is maximal at $\alpha = \pi/4$. Clearly, for a close-to-parallel trimer penetration, smaller α values are desirable, especially when the difference of partial cross sections is appreciable.

The cross sections to Eq. (5) are [6] given by the following expressions:

$$\sigma_{\rm tr}^{\parallel}(k_F) = \frac{3}{4\pi}\int d\Omega_{\mathbf{k}_F}\int d\Omega_{\mathbf{k}'_F}\left(\cos\theta_{\mathbf{k}_F} - \cos\theta_{\mathbf{k}'_F}\right) \times \cos\theta_{\mathbf{k}_F}\,|F(\mathbf{k}_F,\mathbf{k}'_F)|^2, \tag{6}$$

$$\sigma_{\rm tr}^{\perp}(k_F) = \frac{3}{4\pi}\int d\Omega_{\mathbf{k}_F}\int d\Omega_{\mathbf{k}'_F}\,\sin^2\theta_{\mathbf{k}_F} \times \cos^2\varphi_{\mathbf{k}_F}\,|F(\mathbf{k}_F,\mathbf{k}'_F)|^2. \tag{7}$$

Angle averaging is performed by $d\Omega_{\mathbf{k}} = d\varphi_{\mathbf{k}}\sin\theta_{\mathbf{k}}d\theta_{\mathbf{k}}$, where $\varphi_{\mathbf{k}} \in [0,2\pi]$ and $\theta_{\mathbf{k}} \in [0,\pi]$. The above expressions are valid at low velocities, $v < v_F$, where the spherical modeling of a single-center field is reasonable since neither the charge-changing [16,17] nor the wake [18] effects are important there. Furthermore, as was analyzed earlier in detail, the proximity effect in stopping ratios is well characterized by an s-type scattering off such a center [6].

A. Impulse approximation: Role of wave interference

When the $a_{1,2} = a_{2,3} \equiv e^{ikd}/d$ and $a_{1,3} \equiv e^{i2kd}/(2d)$ complex quantities in Eq. (4) are taken equal to zero (impulse approximation), the whole calculation becomes quite simple for a linear trimer $N = 3$. The results derived within our framework for the ratio functions are denoted as $R_N^{\parallel}$ at $\alpha = 0$, and $R_N^{\perp}$ at $\alpha = \pi/2$. In the impulse approximation they are

$$R_N^{\parallel} = 1 + \frac{6}{N}\sum_{n=1}^{N-1}(N-n)\left[j_0^2(nx) - j_1^2(nx) - \frac{2}{nx}\,j_0(nx)j_1(nx)\right], \tag{8}$$

$$R_N^{\perp} = 1 + \frac{6}{N}\sum_{n=1}^{N-1}(N-n)\,\frac{1}{nx}\,j_0(nx)j_1(nx), \tag{9}$$

for arbitrary N in a *linear* chain. Here we introduced $x \equiv k_F d$ and the Bessel functions j_l of the first kind. At a prefixed $x = \pi$ value, we can analytically derive from Eq. (8) the form

$$\sigma_{\rm tr}^{\parallel} \simeq \left[N\left(\frac{4\pi}{k_F^2}\right)\sin^2\eta\right]\left(\frac{1}{N}\,\ln N\right), \tag{10}$$

in leading-order for $N \gg 1$. This, only logarithmic, behavior corresponds to $d = \lambda_F/2$, in terms of the de Broglie wavelength $\lambda_F = 2\pi/k_F$ of an electron with Fermi wave number k_F.

The other component, and thus the average, behaves as $\sigma_{\rm tr}^{\perp} \propto N$, at $x = \pi$. It is tempting to interpret, *a priori*, a complete alignment *together* with the resulting reduced stopping in Eq. (10) above, as a probable realization of the geometrical and energetic intactness. It should be noted that a growing reduction found in the R_N functions by growing N is common in perturbative consideration of the scattering process. Qualitatively similar effects are shown in Fig. 5 in Ref. [1] and Fig. 6 in Ref. [2] for angle-averaged quantities.

Now, we use $N = 3$ and $N = 2$ in Eqs. (8) and (9) to get a perturbative trimer and dimer comparison. In Fig. 1 we exhibit the ratio functions R_N^i. Their properly averaged sum [see, Eq. (5)] characterizes the random situations. The upper panel refers to $N = 3$, while the lower one to the $N = 2$ case. All curves are based on the above-outlined impulse approximation. One can see that in the formal $x \to 0$ case, which must correspond to the $k_F \to 0$ mathematical limit at a physically reasonable finite d value, one gets from Eqs. (8) and (9) simply the number N of independently treated constituents. In the realistic range, where $x \in [1.5,4]$, the $R_N^{\parallel}$ ratios show strong reductions, i.e., notable negative proximity effects.

Unfortunately, at the $x \simeq 3$ value, which fits [6] to the experimental [1] situation with carbon trimer ($d \simeq 2.46$ and $k_F \simeq 1.2$), we get $(R_3^{\parallel}/R_2^{\parallel}) \simeq (2/3)$ and $\mathcal{R}_{3,2} \simeq 1$. These values are in disagreement with the data outlined in Sec. I. Thus, at this level of understanding, we have to conclude that wave-interference effects alone are not enough to get realistic estimations for low-velocity trimer intruders. Within the framework of the applied theoretical method, we should go further in order to get more reliable *a posteriori* statements on the capability of a strong-scattering treatment employed to a linear multicenter intruder.

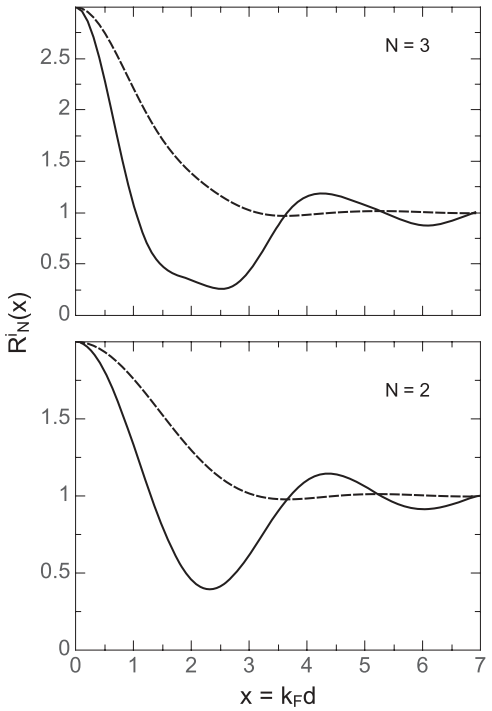

FIG. 1. Illustrative dimensionless ratios R^i_N showing the orientation dependence of renormalized stopping powers of a degenerate electron gas for a slow homonuclear linear trimer ($N = 3$) and dimer ($N = 2$) under parallel ($\parallel$) (solid curves) and perpendicular ($\perp$) (dashed curves) conditions of traversing the target material. The curves are exhibited for the $x \in [0,7]$ mathematical range, where $x = k_F d$. They are calculated from Eqs. (8) and (9), i.e., by neglecting the effect of multiple scattering, but considering wave interference.

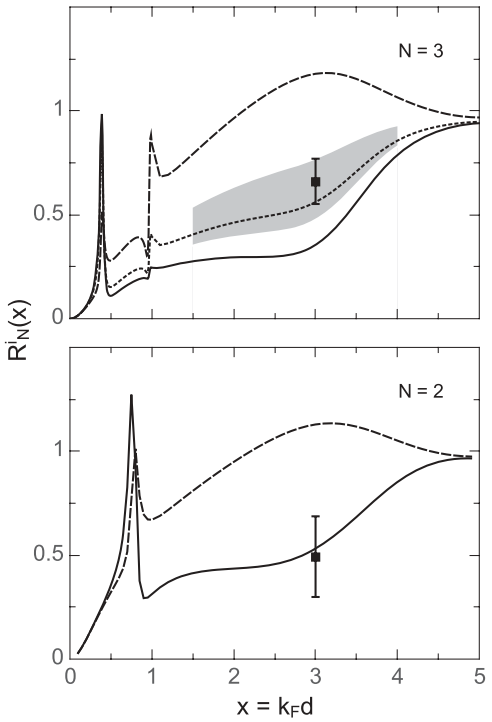

FIG. 2. Dimensionless ratios R^i_N showing the orientation dependence of renormalized stopping powers of a degenerate electron gas for a slow linear carbon trimer ($N = 3$) and dimer ($N = 2$). The conventions of Fig. 1 are used. The dotted curve in the upper panel is based on Eq. (11). The curves are computed by considering wave interference and multiple scattering simultaneously. The shadowed area around the dotted curve brackets the $\alpha \in [\pi/8,\pi/4]$ angle interval. The effective [6,19] phase shift employed is $\eta = 2.3$. The experimental data (with error bars) are exhibited by filled squares. See the text for further details.

B. Role of multiple-electron scattering and interference

Now we investigate the combined effect of wave interference and multiple-electron scattering. Our computation rests on a properly designed code, with N, $a_{1,2}$, $a_{1,3}$, k_F, d, and η as input parameters, that allows a case-to-case study. In Fig. 2, we exhibit the obtained results by using the *same* notation (R^i_N) for the ratio functions as in Fig. 1. Unlike in the case of independent electron scattering, where for the formal $x \to 0$ limit the number of constituents N is obtained, here the behavior is drastically altered. The reason for that stems from the fact that inclusion of multiple-electron scattering [see the second terms in Eq. (4)] strongly modulates the independent-event character of the impulse approximation. Furthermore, in Ref. [6] it was analytically shown for the case of a dimer that the cross sections alone tend to a constant value for fixed d and η at vanishing scattering momenta k_F. Thus, dividing such cross sections by the product $NS_1 \propto N/k_F^2$ one gets zero values for the ratios. For carbon intruders and at the realistic $x = 3$ value, we get $(R^{\parallel}_3/R^{\parallel}_2) \simeq (0.7)$ and $\mathcal{R}_{3,2} \simeq 1$, i.e., about one-half of the data. The comparison of solid curves show the shadow effect discussed in the Introduction.

However, as we mentioned in the Introduction, we have to allow an angle variation in a realistic case with linear trimer of about $(2 \times d) \simeq 5$ a.u. length. With a geometrically reasonable $\alpha = \pi/6$ value, we get for the linear-trimer stopping

$$S(\alpha = \pi/6) = n_0 k_F v \left[\tfrac{3}{4}\sigma^{\parallel}_{\rm tr}(k_F) + \tfrac{1}{4}\sigma^{\perp}_{\rm tr}(k_F)\right]. \quad (11)$$

The ratio $S(\alpha = \pi/6)/[3(4\pi/k_F^2)\sin^2\eta]$ is exhibited on Fig. 2 (upper panel) by a dotted curve. The agreement with experimental data, which is roughly 2/3 at $x = 3$, becomes quite reasonable. The experimental data presented here are obtained after averaging three values plotted in Fig. 4 of Ref. [1]. The shadowed area around the dotted curve, for the realistic $x \in [1.5,4]$ range, marks the corresponding range in the stopping ratio for the $\alpha \in [\pi/8,\pi/4]$ range. Clearly, by allowing a physically constrained range in this angle, we are still around the experimental prediction on trimer stopping. Data with smaller error bars would allow for a better constraint on the angular orientation in our present modeling. With a carbon dimer, an intact transmission is feasible without further geometrical constraint.

The remarkable constancy of the parallel component over a large range of x could have an impact on the proper interpretation of interesting experimental findings [7,9] with H_2^+ intruders. The accurate (with error bar) data sets in Fig. 4 of Ref. [7] for $v \leqslant 0.5$ and in Fig. 3 of Ref. [9] for $v \leqslant 1.5$ show a robust velocity independence of the stopping ratio. We argue that the mentioned constancy found within our nonperturbative

framework could play a decisive role in theoretical modeling of such a behavior in velocity. Indeed, when the dimensionless variable becomes $x = v_r\, d$, where the relative [20] velocity is given by $v_r(x) = v_F[(x+1)^3 - |x-1|^3]/(6x)$ with $x = (v/v_e)$ and $v_e \in [0, v_F]$, the important parallel component would still be small. For instance, $v_r(x=1) = (4/3)v_F$ only.

III. SUMMARY AND OUTLOOK

In this theoretical study we have applied a standard multiple-scattering method in order to quantify the retarding force components experienced by a slow linear carbon trimer moving through a degenerate electron gas. The comparison of results obtained in the impulse approximation within the framework of the method with those obtained without this additional restriction shows that realistic, quantitative estimations cannot be based on oversimplified perturbative approximations. The interference of single-center scattered waves and the role of complex translation operators encoding the modulating effect of multiple scattering are found to be important. The proper weighting of the such obtained orientation-dependent scattering characteristics, governed by an obvious geometrical constraint in the case of a solid-state target, gives a quite reasonable agreement with experimental data.

Based on stationary scattering methods, currently we are working on the two-dimensional (2D) extension of the underlying [21] framework for in-plane chains of atoms as well. The controllable depositions and orientation manipulations of multicenters on close-packed noble metal surfaces represent a direct and real challenge of broad technological relevance. Clearly, the 2D version of the remarkable minimal behavior found for the parallel situation in the present three-dimensional modeling could be vital not only in 2D transport on noble metals but also in the new class of materials [22] with topologically protected 2D surface states. The same scattering characteristics which determine the retarding force in slow-projectile motion in an electron gas are behind the resistivity in transport situations.

ACKNOWLEDGMENTS

We thank P. M. Echenique and J. E. Valdés for very useful discussions. I.N. acknowledges the warm hospitality at the DIPC. This work was supported by the Spanish MICINN (Project No. FIS20010-19609-C02-02).

[1] Y. Takahashi, T. Hattori, and N. Hayashizaki, Phys. Rev. A **75**, 013202 (2007).
[2] P. Sigmund, I. S. Bitensky, and J. Jensen, Nucl. Instrum. Methods B **112**, 1 (1996).
[3] D. Porezag, Th. Frauenheim, Th. Köhler, G. Seifert, and R. Kaschner, Phys. Rev. B **51**, 12947 (1995), especially Table III.
[4] A. Van Orden and R. J. Saykally, Chem. Rev. **98**, 2313 (1998).
[5] S. Heredia-Avalos, R. Garcia-Molina, and I. Abril, Phys. Rev. A **76**, 012901 (2007).
[6] I. Nagy and I. Aldazabal, Phys. Rev. A **81**, 052901 (2010), and references therein.
[7] J. E. Valdés, C. Parra, J. Díaz-Valdés, C. D. Denton, C. Agurto, F. Ortega, N. R. Arista, and P. Vargas, Phys. Rev. A **68**, 064901 (2003).
[8] C. D. Denton, J. Díaz-Valdés, J. E. Valdés, P. Vargas, and N. R. Arista, Nucl. Instrum. Methods B **230**, 36 (2005).
[9] S. M. Shubeita, M. A. Sortica, P. L. Grande, J. F. Dias, and N. R. Arista, Phys. Rev. B **77**, 115327 (2008).
[10] N. R. Arista, Nucl. Instrum. Methods B **164–165**, 108 (2000), and references therein.
[11] Yu. N. Demkov and V. N. Ostrovskii, *Zero-Range Potentials and Their Applications in Atomic Physics* (Plenum, New York, 1988).
[12] R. Szmytkowski and M. Gruchowski, Phys. Rev. A **70**, 062719 (2004).
[13] N. F. Mott and S. W. Massey, *The Theory of Atomic Collisions* (Clarendon, Oxford, 1965).
[14] H. M. Urbassek, V. Dröge, and R. M. Nieminen, J. Phys.: Condens. Matter **5**, 3289 (1993).
[15] R. Díez Muiño and A. Salin, Phys. Rev. B **62**, 5207 (2000).
[16] F. Guinea, F. Flores, and P. M. Echenique, Phys. Rev. B **25**, 6109 (1982).
[17] P. M. Echenique, I. Nagy, and A. Arnau, Int. J. Quantum Chem. Quantum Chem. Symp. **23**, 521 (1989).
[18] A. Mazarro, P. M. Echenique, and R. H. Ritchie, Phys. Rev. B **27**, 4117 (1983).
[19] M. J. Puska and R. M. Nieminen, Phys. Rev. B **27**, 6121 (1983).
[20] S. Kreussler, C. Varelas, and W. Brandt, Phys. Rev. B **23**, 82 (1981).
[21] I. Nagy, Phys. Rev. B **82**, 155439 (2010), and references therein.
[22] M. Z. Hasan and C. L. Kane, Rev. Mod. Phys. **82**, 3045 (2010).